openheart

High afterload rather than myocardial fibrosis predicts reduced ejection fraction in severe aortic stenosis with afterload mismatch

Megan Rian Rajah , Anton Doubell, Philip Herbst

To cite: Rajah MR, Doubell A, Herbst P. High afterload rather than myocardial fibrosis predicts reduced ejection fraction in severe aortic stenosis with afterload mismatch. *Open Heart* 2025;**12**:e003345. doi:10.1136/openhrt-2025-003345

Received 27 March 2025
Accepted 20 April 2025

Cardiology, Medicine, Stellenbosch University, Cape Town, Western Cape, South Africa

Correspondence to
Dr Megan Rian Rajah;
meganrajah@yahoo.com

ABSTRACT

Background Afterload mismatch (AM) refers to high-gradient (mean gradient ≥40 mm Hg) severe aortic stenosis (AS) with reduced left ventricular ejection fraction (LVEF <50%) that is hypothesised to arise from mechanisms other than true contractile impairment. The extent, pattern and functional impact of myocardial fibrosis (MF), which is associated with systolic impairment, is poorly understood in the context of AM.

Methods High-gradient severe AS patients with (n=25; low ejection fraction high-gradient, LEF-HG) and without (n=33; normal ejection fraction high-gradient (NEF-HG)) reduced LVEF underwent cardiovascular MRI. Using T1 mapping, extracellular volume (ECV) fraction and late gadolinium enhancement (LGE), the extent and pattern of MF was compared between the two groups. End-systolic wall stress (ESWS) as a measure of afterload was estimated, and its relationship with LVEF was compared with that of MF and LVEF.

Results Stenosis severity was worse in the LEF-HG group (aortic valve area 0.5±0.2 vs 0.7±0.2 cm^2, mean gradient 55 (46–66) vs 48 (41–69) mm Hg). In the LEF-HG group, high ESWS with cavity dilation and significant hypertrophy were observed compared with the NEF-HG group. MF was present in both groups with a significantly higher burden in the LEF-HG group (T1 time 1061±22 vs 1041±33 ms, ECV 26%±3% vs 24%±3%, LGE mass 4.3 (1.7–9.3) vs 0.1 (0.06–3.39) g). The association between MF and LVEF was weak, while ESWS was strongly associated with LVEF (r −0.8, p<0.0001) and was the best predictor of LVEF in multivariate prediction analysis.

Conclusions MF was present in both groups with a higher burden in those with LEF-HG AS. High ESWS, that is, afterload, rather than MF, was the strongest predictor of LVEF. While MF may not directly impact systolic function in AM, it is still an important factor to account for in AS given its association with increased mortality.

WHAT IS ALREADY KNOWN ON THIS TOPIC

⇒ The reduced left ventricular ejection fraction (LVEF) in afterload mismatch likely arises from mechanisms other than true intrinsic contractile dysfunction of the cardiomyocytes given the ability of the left ventricle to maintain high transaortic pressure gradients in the severe range (mean gradient ≥40 mm Hg).

WHAT THIS STUDY ADDS

⇒ The myocardial fibrosis burden is higher in those with afterload mismatch compared with patients with normal ejection fraction high-gradient aortic stenosis (AS), but fibrosis is not a strong predictor of LVEF in these patients.

⇒ Increased afterload measured by end-systolic wall stress is the strongest predictor of LVEF in high-gradient severe AS, reaffirming initial hypotheses that the abnormal loading conditions are what lead to a reduced LVEF.

⇒ The increased myocardial fibrosis burden may, however, be a marker of chronicity in high-gradient AS, therefore, conferring other important clinical implications, for example, an increased mortality risk.

HOW THIS STUDY MIGHT AFFECT RESEARCH, PRACTICE OR POLICY

⇒ Further study is required to establish whether myocardial fibrosis, which is associated with worse outcomes, is a marker of chronicity in AS. Understanding this will help policy-makers define and update criteria for the optimal timing of valve intervention, thus improving long-term survival and outcomes in AS patients.

INTRODUCTION

Severe aortic stenosis (AS) is one of the most common valve lesions worldwide with a high mortality despite advances in interventional options (surgical aortic valve replacement (SAVR) and transcatheter aortic valve implantation (TAVI)).[1] Several haemodynamic subtypes of severe AS have been described, and mortality appears to be higher in those with low ejection fraction high-gradient (LEF-HG) severe AS, or afterload mismatch, compared with their normal ejection fraction high-gradient (NEF-HG) counterparts.[2] Afterload mismatch is a poorly understood haemodynamic subtype of severe AS first described in the 1970s.[3–5] It refers to those high-gradient severe AS patients with a

reduced left ventricular ejection fraction (LVEF <50%) that is thought to arise from a combination of inadequate left ventricular (LV) remodelling and abnormal loading conditions, that is, high afterload, rather than true contractile dysfunction of the cardiomyocytes.[3–5] This hypothesis was, however, derived prior to the histological descriptions of myocardial fibrosis in severe AS.[6 7]

Myocardial fibrosis is now well described in AS and presents itself in the form of two distinct patterns detectable on cardiovascular MR (CMR) imaging—diffuse interstitial fibrosis detected by T1 mapping/extracellular volume (ECV) fraction, and replacement fibrosis detected by late gadolinium enhancement (LGE) imaging.[8 9] There is strong evidence to suggest that myocardial fibrosis is associated with an increased mortality risk in severe AS and that its progression coincides with the transition to systolic dysfunction and heart failure.[7] How myocardial fibrosis impacts systolic function is not well understood, but limited evidence suggests that it may disrupt essential myocyte-to-myocyte communication that is required for cardiomyocyte homeostasis and survival, as well as excitation–contraction coupling disruption by physically restricting the cardiomyocytes from thickening.[10] Myocardial fibrosis in afterload mismatch is not well characterised and its contribution to the reduced LVEF is not known.

This study aimed to describe, quantify and compare the myocardial fibrosis burden between patients with afterload mismatch (LEF-HG AS) and those with high-gradient severe AS and preserved LVEF (NEF-HG AS) using CMR. To better understand the relative impact of myocardial fibrosis on preintervention LVEF, end-systolic wall stress (ESWS) as a measure of afterload was calculated non-invasively, and both ESWS and fibrosis were correlated with LVEF.

METHODS

Study design

Between June 2021 and August 2024, 58 patients meeting the European Society of Cardiology's criteria[11] for high-gradient severe AS were prospectively enrolled from a tertiary academic centre in the Western Cape, South Africa. These criteria included an aortic valve area (AVA) <1.0 cm^2 and a mean transaortic pressure gradient ≥40 mm Hg. Patients with additional haemodynamically significant valvular lesions, comorbid structural heart diseases including amyloidosis, significant coronary artery disease (>50% stenosis determined by coronary angiography) and contraindications to CMR were excluded. A clinical history with details on symptoms, functional status in the form of a New York Heart Association class and comorbidities were recorded. A resting blood pressure and clinical features of heart failure were also determined through a clinical examination. Echocardiography was performed to determine LVEF, AVA and transvalvular aortic gradients to classify patients into their respective study groups (LEF-HG vs NEF-HG using an LVEF cut-off of 50%). Coronary angiography was performed to exclude significant coronary artery disease. All participants then underwent CMR using a standardised protocol described below.

CMR image acquisition

CMR imaging was performed at Tygerberg Hospital using a Siemens Magnetom Aera 1.5 Tesla scanner (Siemens, Erlangen, Germany). A standardised protocol in accordance with the Society of Cardiovascular Magnetic Resonance guidelines was used.[12] Cine images in the standard cardiac planes (two-chamber, three-chamber and four-chamber views as well as a short-axis stack) were acquired using an electrocardiogram-gated, breath-held, balanced steady-state free precession sequence. Typical cine image acquisition parameters included an 8 mm slice thickness with a 2 mm gap where applicable, 25 phases, TR 35–45 ms, TE 1.2 ms. Through-plane phase contrast flow at the aortic valve tips was also acquired with typical parameters that included a 5 mm slice thickness, 50 phases, TR 26 ms, TE 3.71 ms and velocity encoding of 400–550 cm/s.

Native and postcontrast T1 mapping images were acquired using a modified look-locker inversion recovery 5 (3)3 acquisition scheme. Native T2 mapping was performed using a T2 magnetisation preparation pulse and a readout by means of true fast imaging with steady state precession. Image views for the parametric sequences included a three-slice short axis stack (a basal, mid and apical slice of the LV) and the standard two-chamber, three-chamber and four-chamber views. The short axis stack was acquired using the five-three rule to ensure consistency across participants. Typical parameters included an 8 mm slice thickness with TR 290 ms/TE 1.1 ms for native T1 mapping, TR 343 ms/TE 1.1 ms for postcontrast T1 mapping and TR 214 ms/TE 1.2 ms for T2 mapping. Normal mapping reference ranges were previously established in a calibration study of normal participants (TygerHeart MAPCAL Study, N21/02/005).

Contrast imaging was performed using Gadovist (Bayer Pharmaceuticals, Leverkusen, Germany) contrast agent at a dose of 0.2 mmol/kg. LGE images were acquired 10–12 min after contrast injection using a T1-weighted inversion recovery sequence. The LGE images were acquired as a short-axis stack covering from base to apex of the LV and in the standard two-chamber, three-chamber and four-chamber views. Typical LGE image parameters included a slice thickness of 8 mm with a gap of 2.5 mm where applicable, TR 806 ms, TE 1 ms, and inversion times ranging between 240 and 280 ms (as guided by a modified look-locker TI scout image).

CMR image analysis

Images were analysed using CVI42 (V.5.13.7, Circle Cardiovascular Imaging, Canada) software. A volumetric and functional analysis of the LV was performed in accordance with the Society of Cardiovascular Magnetic Resonance's guidelines.[13] A semiautomated volumetric and functional analysis was performed by

contouring end-diastolic and end-systolic endocardial and epicardial borders in every slice of the short-axis cine stack. Trabeculations and papillary muscles were excluded from the blood pool. Reported parameters include LV end-diastolic volume (LVEDV), LV end-systolic volume, LV stroke volume (LVSV), LVEF and mitral annular plane systolic excursion (MAPSE). The letter, 'i' denotes parameters indexed for Mostellar-derived body surface area. Right ventricular volumes were derived similarly and are denoted by the letters 'RV'. ESWS was calculated non-invasively using the equation derived and validated by Reichek *et al*.[14] LV pressure was estimated using the sum of systolic blood pressure and mean transaortic pressure gradient, and geometric measurements were performed using the method suggested by Carter-Storch *et al*.[15] Flow rate was calculated by dividing the LVSV by the systolic ejection time derived from aortic valve phase contrast flow curves. The LV global function index (LVGFI), described by Mewton *et al*, was calculated by dividing the LVSV by the sum of the mean cavity size (half the sum of LVEDV and LVESV) and myocardial volume (LVM divided by 1.05 g/mL).[16]

Global T1 and T2 relaxation times were measured using the three-slice short-axis stacks. Endocardial and epicardial borders were contoured on every slice of the stack using a 10% endocardial and epicardial offset to account for partial volume effects. The average T1 and T2 times for the three slices were then used as global measures of T1 and T2 relaxation time. The right ventricular insertion points were marked to generate a segmental (American Heart Association 17 segment model)[17] analysis of the T1 and T2 relaxation times across each segment of the LV. The previously validated equation below was used to calculate the ECV fraction[18]:

$$ECV = \left[\frac{\Delta R1_{myocardium}}{\Delta R1_{LV\ blood\ pool}}\right] \times \left[1 - sHCT\right]$$

Where:

ΔR1=postcontrast T1 time–precontrast T1 time

sHCT=synthetic haematocrit

A synthetic haematocrit was calculated for the ECV calculation using the validated formula below[19]:

$$sHCT = \left[866 \times \frac{1}{T1_{LV\ blood\ pool}}\right] - 0.1232$$

Where:

$T1_{LV\ blood\ pool}$=Native T1 relaxation time of blood pool

The LGE images were analysed qualitatively and quantitatively. The presence and pattern (infarct vs non-infarct) of LGE were determined visually. For the quantitative analysis, endocardial and epicardial contours were traced in every slice of the short-axis LGE stack. Using an overlay slider and visual guidance, the LGE mass and proportion were recorded. Based on the best current evidence, a semiautomated quantitative analysis was also performed using the signal threshold versus reference mean method at a threshold of 3 SDs above that of remote myocardium.[20]

Statistical analysis

Statistical analysis was performed using GraphPad Prism (V.10.0.2, GraphPad, Boston, USA) and SPSS (V.30.0, IBM) for statistical analysis. A minimum sample size of 12 participants per group was required and met for the detection of volumetric and mass differences of at least 10 mL and 10 g, respectively, with a power of 95% at an alpha of 5%. To detect a mean difference in T1 relaxation time of 20 ms and in LGE mass of 10 g with a power of 80% at an alpha of 5%, 33 and 8 participants, respectively were required. Categorical variables were presented as absolute number and percentage and were compared using the χ^2 test. Continuous variables were tested for normality using the Shapiro-Wilk test. Normally distributed continuous variables were presented as means and SDs and compared using the Student's t-test. Continuous variables not normally distributed were presented as medians and IQRs and were compared using the Mann-Whitney U test. A $p<0.05$ was considered significant. Pearson and Spearman correlation analyses were used for normally and non-normally distributed data, respectively. Prediction analyses using simple linear regression and general discriminant analysis were also performed.

RESULTS

Baseline characteristics

Of 58 recruited participants with high-gradient severe AS, 25 (43%) had LEF-HG AS and the remaining 33 (57%) had NEF-HG AS (table 1). The mean ages in those with LEF-HG and NEF-HG AS were 59±14and 63±8 years, respectively. The majority of the cohort (40 (69%)) were female with a similar sex distribution in each group (table 1). In those with LEF-HG AS, a significantly smaller AVA (0.5±0.2 vs 0.7±0.2 cm^2) was observed. Mean and peak pressure gradients were statistically similar between the two groups (table 1) but with a significantly lower flow rate in those with LEF-HG AS (182.5±71.1 vs 265.9±69.3 mL/s) (table 1). With the exceptions of dyspnoea, orthopnoea and systolic blood pressure, the clinical characteristics of the two groups were similar (table 1). There were no cases of concomitant amyloidosis. Of 25 LEF-HG AS patients, 18 (72%) underwent valve intervention by either SAVR or TAVI. Transthoracic echocardiography performed 4–7 days after intervention confirmed LVEF recovery in 14/18 (78%) patients. The median improvement in LVEF was 12.5 (2.5%–19%).

LV morphology/geometry/function

LV remodelling and functional parameters were significantly different between the two groups of patients (table 2). LV remodelling in LEF-HG AS included significant cavity dilation compared with those with NEF-HG AS (LVEDV 221.1±52.9 vs 148.4±31.1 mL) as well as significant LV hypertrophy (LVM 181.5±61.4 vs 147.4±47.4 g). Measures of both radial and longitudinal systolic function were moderate-severely impaired in the LEF-HG AS group (LVEF 28%±8% vs 65%±9%, $p<0.0001$ and MAPSE

Table 1 Baseline characteristics of LEF-HG AS compared with NEF-HG AS patients

Characteristic	LEF-HG (n=25)	NEF-HG (n=33)	P value
Age (years)	59±14	63±8	0.2
Sex			0.9
Female n (%)	17 (68)	23 (70)	
Male n (%)	8 (32)	10 (30)	
AVA (cm^2)	0.5±0.2	0.7±0.2	**0.0005**
Mean gradient (mm Hg)	55 (46–66)	48 (41–69)	0.5
Peak gradient (mmHg)	89 (72–107)	74 (66–104)	0.3
Flow rate (mL/s)	182.5±71.1	265.9±69.3	**<0.0001**
Symptoms			
Chest pain n (%)	11 (44)	11 (33)	0.3
Dyspnoea n (%)	24 (96)	20 (61)	**0.002**
NYHA			
Class I n (%)	0 (0)	1 (3)	0.4
Class II n (%)	8 (32)	7 (21)	0.3
Class III n (%)	14 (56)	11 (33)	0.08
Class IV n (%)	2 (8)	1 (3)	0.4
Orthopnoea n (%)	15 (60)	10 (30)	**0.02**
Pre-syncope n (%)	13 (52)	12 (36)	0.2
Syncope n (%)	7 (28)	9 (27)	0.9
Comorbidities			
Hypertension n (%)	14 (56)	23 (70)	0.3
Diabetes mellitus n (%)	4 (16)	10 (30)	0.2
Dyslipidaemia n (%)	5 (20)	12 (36)	0.2
Coronary artery disease n (%)	0 (0)	0 (0)	N/A
Cardiac amyloidosis* n (%)	0 (0)	0 (0)	N/A
Clinical features			
Heart rate (beats per minute)	82±14	71±14	**0.004**
Systolic blood pressure (mm Hg)	115±21	132±19	**0.002**
Diastolic blood pressure (mm Hg)	72±9	73±13	0.6
Body mass index (kg/m^2)	27.6±6.6	31.1±7.1	0.06
Body surface area (m^2)	1.8±0.2	1.9±0.2	0.2
Baseline LVEF	28±8	65±9	**<0.0001**

Categorical variables are presented as absolute number (percentage).
Normally distributed continuous variables are presented as mean±SD and median (IQR) where distribution is not normal.
Statistically significant p values illustrated in bold (p<0.05 considered significant).
*Incidentally detected amyloidosis as per CMR features.
AS, aortic stenosis; AVA, aortic valve area; CMR, cardiovascular MR; LEF-HG, low ejection fraction high gradient; LVEF, left ventricular ejection fraction.; N/A, not available; NEF-HG, normal ejection fraction high gradient; NYHA, New York Heart Association.

3.7±2.6 vs 10.2±3.4 mm, p<0.0001). Non-invasive meridional ESWS was significantly higher in the LEF-HG AS group (263.6±82.2 vs 118.3±49.5×10^3 dynes/cm^2). The conical shape of the LV was equally preserved in both groups of patients (sphericity index of 0.5±0.1 vs 0.5±0.1). The novel index of LV global function was significantly decreased in the LEF-HG AS group (LVGFI 17.4±5.4 vs 41.2±8.9).

LV tissue characteristics

Myocardial fibrosis measured by T1 mapping, ECV and LGE was present in both groups of patients (table 3). The global T1 relaxation time was significantly longer in the LEF-HG group (1061±22 vs 1041±33 ms; normal T1 range 1000±23 ms). The impact of heart rate on the T1 relaxation time was shown to be insignificant on simple linear regression analysis (r^2=0.0097). The ECV was significantly increased in LEF-HG AS (26%±3% vs 24%±3%; normal ECV 23%±2%). The global T2 relaxation time was identical between the two groups (normal T2 range 47±2 ms). A segmental analysis of T1 mapping is shown in figure 1. A similar distribution of prolonged T1 relaxation time was observed between the two groups, with the highest T1 values distributed in the inferior and septal segments.

The incidence of replacement fibrosis as determined by the presence of LGE was significantly higher in those with LEF-HG AS (84% vs 36%) and in both groups, a non-infarct pattern of LGE predominated over an infarct pattern (table 3). The scar burden was higher in those with LEF-HG AS with a total segment count of 61 (15%) vs 46 (9%), p=0.003 and a significantly higher LGE mass using both visual planimetry and the 3SD STRM method (table 3). A basal to apical gradient in terms of scar burden was observed in LEF-HG AS, with the greatest number of LGE positive segments in the basal third of the ventricle. This gradient was less apparent in those with NEF-HG AS (table 3).

Relationship between ESWS and myocardial fibrosis

ESWS was not uniformly distributed across the LV. For the total cohort, ESWS measured highest in the middle third of the LV, measuring 208.0±77.9×10^3 dynes/cm^2 compared with 182.0±97.7 and 138.7±76.3×10^3 dynes/cm^2 in the basal and apical thirds of the LV, respectively. This contrasts with the decreasing density of fibrosis from base to apex observed in the LV. In those with an abnormally elevated T1 relaxation time (46 (79%)), concordance between the basal to apical distributions of ESWS elevation and fibrosis density was present in only 8 (17%) of the patients (p=0.0002). Similarly, in those with LGE present, concordance between the basal to apical distributions of ESWS elevation and fibrosis density was present in only 11 (33%) of the patients (p=0.12). The strength of association between ESWS and global native T1 relaxation time was weak on Spearman correlation analysis (r=0.15, 95% CI −0.12 to 0.40, p=0.2). Similarly, a weak association was found between ESWS and LGE mass (r=0.27, 95% CI 0.003 to 0.50, p=0.04).

Table 2 Left and right ventricular remodelling in those with LEF-HG AS compared with NEF-HG AS

Parameter	LEF-HG (n=25)	NEF-HG (n=33)	P value
LVEDV (mL)	221.1±52.9	148.4±31.1	**<0.0001**
LVEDVi (mL/m^2)	122.6±31.6	77.8±15.5	**<0.0001**
LVESV (mL)	160.6±46.5	51.8±17.5	**<0.0001**
LVESVi (mL/m^2)	88.4±25.8	27.2±9.6	**<0.0001**
LVSV (mL)	61.3±20.6	96.7±23.5	**<0.0001**
LVSVi (mL/m^2)	34.1±13.4	50.5±11.2	**<0.0001**
Flow rate (mL/s)	182.5±71.1	265.9±69.3	**<0.0001**
LVM (g)	181.5±61.4	147.4±47.4	**0.03**
LVMi (g/m^2)	100.1±37.5	76.6±21.6	**0.008**
M/V ratio	0.8±0.2	1.0±0.3	**0.009**
SI	0.5±0.1	0.5±0.1	0.1
LVEF (%)	28±8	65±9	**<0.0001**
MAPSE (mm)	3.7±2.6	10.2±3.4	**<0.0001**
Meridional ESWS (×10^3 dynes/cm^2)	263.6±82.2	118.3±49.5	**<0.0001**
LVGFI	17.4±5.4	41.2±8.9	**<0.0001**
RVEDV (mL)	130.8 (113.7–189.1)	139.0 (107.0–154.5)	0.4
RVEDVi (mL/m^2)	73.8 (60.1–104.8)	68.3 (56.5–80.2)	0.1
RVESV (mL)	62.6 (50.6–101.6)	49.9 (37.8–63.3)	**0.003**
RVESVi (mL/m^2)	36.1 (30.0–59.0)	26.3 (20.5–30.4)	**0.0002**
RVSV (mL)	67.9 (52.9–80.0)	77.8 (63.8–99.0)	0.05
RVSVi (mL/m^2)	36.5 (28.5–43.5)	39.5 (35.4–50.0)	0.09
RVEF (%)	48±12	61±8	**<0.0001**
TAPSE (mm)	15±5	21±5	**<0.0001**
TR present n (%)	7 (28)	2 (6)	**0.02**

Categorical variables are presented as absolute number (percentage).
Normally distributed continuous variables are presented as mean±SD and median (IQR) where distribution is not normal.
Statistically significant p values illustrated in bold (p<0.05 considered significant).
The letter 'i' denotes a parameter indexed to body surface area.
AS, aortic stenosis; ESWS, end-systolic wall stress; LEF-HG, low ejection fraction high gradient; LVEDV, left ventricular end-diastolic volume; LVEF, left ventricular ejection fraction; LVESV, left ventricular end-systolic volume; LVGFI, left ventricular global function index; LVM, left ventricular mass; LVSV, left ventricular stroke volume; MAPSE, mitral annular plane systolic excursion; M/V, mass/volume ratio; NEF-HG, normal ejection fraction high gradient; RVEDV, right ventricular end-diastolic volume; RVEF, right ventricular ejection fraction; RVESV, right ventricular end-systolic volume; RVSV, right ventricular stroke volume; SI, sphericity index; TAPSE, tricuspid annular plane systolic excursion; TR, tricuspid regurgitation.

Predictors of afterload mismatch

Pearson and Spearman correlation analyses showed a significant weak association between markers of fibrosis and LVEF (T1 time: r=−0.35, 95% CI −0.56 to −0.10, p<0.01, ECV: r=−0.34, 95% CI −0.59 to −0.03, p=0.03 and LGE mass: r=−0.42, 95% CI −0.62 to −0.17, p=0.001). ESWS, however, had a strong inverse linear association with LVEF (r=−0.80, 95% CI −0.88 to −0.67, p<0.0001). On univariate linear regression analysis, T1 time and ESWS were found to have significant unstandardised β coefficients for the prediction of LVEF (table 4). The standardised β coefficient was strongest for ESWS (table 4). Using a general discriminant analysis for a multivariate evaluation, LGE mass and ESWS were found to have significant β coefficients for the prediction of LVEF (table 4). As for univariate analysis, ESWS had a stronger β coefficient than LGE mass (table 4). The model accurately predicted LV systolic dysfunction with a high sensitivity of 90% and specificity of 95%.

DISCUSSION

This study comparing patients with LEF-HG AS to their NEF-HG counterparts found more advanced LV remodelling (in the form of LV dilation and LV hypertrophy) with significantly elevated ESWS in those with LEF-HG AS. The diffuse interstitial and replacement fibrosis burden, although present in both groups, was significantly higher in the LEF-HG group. ESWS rather than myocardial fibrosis was a strong predictor of LVEF, suggesting that

Table 3 Left ventricular tissue characteristics of those with LEF-HG AS compared with NEF-HG AS

Parameter	LEF-HG (n=25)	NEF-HG (n=33)	P value
Global T1 time (ms)	1061±22	1041±33	**0.008**
Basal T1 time (ms)	1062±21	1051±38	0.2
Mid T1 time (ms)	1059±28	1037±33	**0.008**
Apical T1 time (ms)	1064±39	1027±36	**0.001**
ECV (%)	26±3	24±3	**0.02**
Global T2 time (ms)	49 (48–49)	49 (47–51)	0.6
Basal T2 time (ms)	49 (47–49)	48 (47–51)	0.5
Mid T2 time (ms)	49±2	49±3	0.8
Apical T2 time (ms)	49 (48–50)	49 (48–51)	0.6
LGE present n (%)	21 (84)	12 (36)	**0.0003**
Basal segments n (%)	27 (18)	17 (9)	**0.009**
Mid segments n (%)	21 (14)	19 (10)	0.2
Apical segments n (%)	13 (13)	10 (8)	0.2
LGE pattern			
Infarct n (%)	5 (24)	5 (42)	0.3
Non-infarct n (%)	16 (76)	9 (75)	0.9
LGE mass (g) by visual method	4.3 (1.7–9.3)	0.1 (0.06–3.4)	**0.002**
LGE percentage (%) by visual method	4.9 (1.4–8.6)	0.1 (0.1–3.9)	**0.002**
LGE mass (g) by 3SD STRM method	14.3 (7.5–20.3)	5.3 (2.2–13.3)	**0.008**
LGE percentage (%) by 3SD STRM method	12.0 (10.1)	7.0 (12.5)	**0.04**

Categorical variables are presented as absolute number (percentage).
Normally distributed continuous variables are presented as mean±SD and median (IQR) where distribution is not normal.
Statistically significant p values illustrated in bold (p<0.05 considered significant).
AS, aortic stenosis; ECV, extracellular volume; LEF-HG, low ejection fraction high gradient; LGE, late gadolinium enhancement; NEF-HG, normal ejection fraction high gradient; STRM, signal threshold versus reference mean.

a mismatch between afterload increase and LV compensation lies at the centre of the reduced LVEF in high-gradient severe AS (ie, an afterload mismatch as initially suggested, exists). The development of myocardial fibrosis appears to be independent of the rise in ESWS, as suggested by the poor correlation between the overall LV fibrosis quantity and ESWS, as well as the lack of concordance between the basal to apical distributions of fibrosis and regional ESWS elevations.

Abnormal loading is a stronger predictor of preintervention systolic dysfunction than myocardial fibrosis

Myocardial fibrosis was present in both groups of patients in this study, suggesting that fibrosis in AS likely precedes the onset of systolic dysfunction as measured by a reduced LVEF. This temporality is an important criterion for establishing a causal relationship between myocardial fibrosis and systolic dysfunction. However, neither a strong association nor a dose-dependency between the fibrosis burden and LVEF was demonstrated in this study. This was true for both diffuse interstitial and replacement fibrosis. Rather, a strong association and dose-dependent effect between ESWS, that is, afterload, and LVEF was observed. This suggests that abnormal loading (more specifically, increased afterload) serves as a stronger causal contender than myocardial fibrosis for the reduced LVEF in afterload mismatch. Further supporting this is the observation of an early LVEF recovery following intervention.[21–23] While regression of diffuse interstitial fibrosis has been described after SAVR/TAVI, this regression appears to be gradual over a period of months and is not as immediate as the acute recovery observed for LVEF.[24–27] A formal analysis of LVEF recovery was not performed in this study and would be an important addition in future work on afterload mismatch to better illustrate the relationship between LVEF recovery and fibrosis regression.

Clinical significance of myocardial fibrosis in afterload mismatch

While the results of this study suggest that myocardial fibrosis may not be causally associated with the reduced LVEF in afterload mismatch, its presence is still of clinical importance given its association with increased mortality. In our cohort of afterload mismatch, more severe degrees of stenosis severity and more advanced LV remodelling suggest that these patients represent a more advanced stage in the natural history of severe AS. It is therefore plausible that myocardial fibrosis, which was also significantly higher in afterload mismatch, may be a marker of chronicity. Despite good evidence of increased mortality associated with myocardial fibrosis in AS, interventional strategies based on selecting patients with worse fibrosis for early surgery have not demonstrated improved outcomes.[28] In the recently completed EVOLVED trial that randomised asymptomatic severe AS patients with midwall LGE to either early intervention or to the current guideline recommendation of conservative management, early intervention did not translate into a significant reduction in the primary endpoint (composite of all-cause mortality and AS-related hospitalisation).[28] This highlights the current knowledge gap with regards to the role of fibrosis assessment in predicting patient outcomes in severe AS.

Long-term considerations in afterload mismatch

The prompt recovery in LVEF after valve intervention in those with afterload mismatch may lead to a false sense of reassurance regarding the long-term outcomes of these patients. Few studies designed to interrogate the intermediate and/or long-term outcomes specifically in those with afterload mismatch exist.[2 29–31] The findings are conflicting. In one study, those with afterload mismatch performed similarly at 1 year compared with those with high-gradient severe AS and preserved

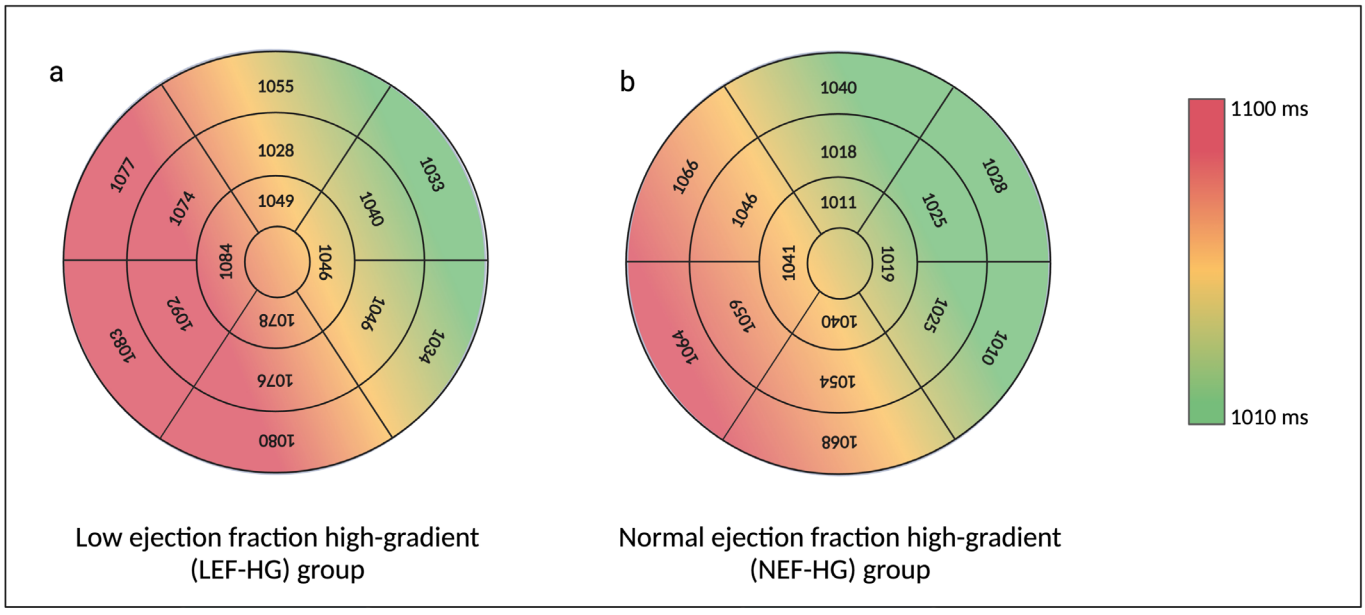

Figure 1 Heat maps showing the segmental distribution of diffuse myocardial fibrosis as detected by global native T1 relaxation time in those with (a) LEF-HG AS and (b) NEF-HG AS. The green regions represent segments with a normal T1 relaxation time (T1 time <1040 ms). The yellow and red regions represent segments with moderate and severe elevations in T1 relaxation time (T1 time: 1040–1100 ms). Septal predominance in terms of myocardial fibrosis was present in both groups of patients. AS, aortic stenosis.

systolic function.[30] In a larger study, however, those with afterload mismatch trended strongly towards a higher cardiovascular mortality at 2 years after valve intervention.[2] Concerns of an increased mortality risk in afterload mismatch are further supported by the presence of a significant fibrosis burden and a drastically lower LVGFI observed in this study. This novel marker, first described by Mewton *et al*, combines structural and functional measures into a single dimensionless index.[16] This index, in other cohorts of cardiovascular disease, has been shown to be a comprehensive tool for the independent long-term prediction of heart failure, cardiovascular events and mortality.[16 32 33] Use of LVGFI in the severe AS population remains unexplored. Given the significant difference in LVGFI between those with afterload mismatch and preserved systolic function, there would be merit in performing longer-term studies and in establishing the utility of this predictive marker in the AS population.

Limitations

Myocardial contractility and preload were measured in only a subset of this study's cohort,[5] and their impact on LVEF in the rest of the cohort was therefore unknown. Although, impaired contractility was not shown to play a significant role in the systolic dysfunction of the afterload mismatch subset who were previously studied.[5] This study design did not include a follow-up arm which would be useful in future work to further clarify the relative contributions of myocardial fibrosis and reverse LV remodelling on LVEF in afterload mismatch.

Table 4 Univariate linear regression and multivariate general discriminant analysis of predictors of left ventricular systolic dysfunction

Predictor variable	Univariate analysis				General discriminant analysis		
	β coefficient	95% CI	Standardised β coefficient	P value	β coefficient	95% CI	P value
T1 time (ms)	−0.16	−0.32 to −0.01	−0.25	**0.04**	0.18	−0.02 to 0.39	0.08
ECV (%)	57.00	−123.69 to 237.68	0.09	0.53	−0.11	−0.36 to 0.14	0.37
LGE mass (g)	−0.54	−1.38 to 0.29	−0.16	0.19	0.28	0.06 to 0.51	**0.01**
ESWS*	−0.17	−0.22 to −0.13	−0.78	**<0.01**	0.8	0.63 to 0.96	**<0.01**

A p<0.05 was considered statistically significant.
Significant p values are denoted by bold text.
*ESWS measured non-invasively and expressed as $\times 10^3$ dynes/cm^2.
ECV, extracellular volume fraction; ESWS, end-systolic wall stress; LGE, late gadolinium enhancement.

CONCLUSIONS

In this CMR-based study of patients with high-gradient severe AS, the degree of diffuse interstitial and replacement fibrosis in afterload mismatch exceeded that of patients with normal EF. Diffuse interstitial fibrosis demonstrated a septal predominance, and a basal to apical gradient in terms of replacement fibrosis was observed. ESWS as a measure of afterload was also shown to be significantly higher in patients with afterload mismatch and was the strongest predictor of LVEF. In keeping with prior hypotheses, abnormal loading (excessive afterload) remains the most likely mechanism underlying the reduced LVEF in this unique subgroup of severe AS patients, but future prospectively designed studies that follow fibrosis regression and LVEF recovery post valve intervention are required to strengthen these findings. While myocardial fibrosis may not play a direct role in systolic dysfunction, its previously established role on increased mortality risk in AS is important and requires further study.

Acknowledgements The authors would like to thank Professor Martin Kidd and Dr. Mohammed Talle for their assistance and support.

Contributors Using the CrediT system, author contributions are summarised as follows: MRR: conceptualisation, methodology, investigation, formal analysis, writing–original draft, review and editing, visualisation. AD: supervision, conceptualisation, methodology, writing–review and editing, resources. PH: supervision, conceptualisation, methodology, writing–review and editing, resources. MRR stands as the guarantor of the article.

Funding This work was enabled through funding from the SUNHEART centre of the Division of Cardiology, Department of Medicine at Tygerberg Hospital/Stellenbosch University and the Harry Crossley Foundation. The degree from which this study emanated was funded by the South African Medical Research Council (SAMRC) through its Division of Research Capacity Development under the SAMRC Clinician Researcher Programme.

Disclaimer The content hereof is the sole responsibility of the authors and does not necessarily represent the official views of the SAMRC.

Competing interests None declared.

Patient consent for publication Not applicable.

Ethics approval This study involves human participants and was approved by Human Research Ethics Committee of Stellenbosch University (Ref: S21/11/251 PHD). Participants gave informed consent to participate in the study before taking part.

Provenance and peer review Not commissioned; externally peer reviewed.

Data availability statement Data are available on reasonable request. Data are available on reasonable request made to the corresponding author.

ORCID iD

Megan Rian Rajah http://orcid.org/0000-0001-5599-6608

REFERENCES

1 Coffey S, Roberts-Thomson R, Brown A, *et al*. Global epidemiology of valvular heart disease. *Nat Rev Cardiol* 2021;18:853–64.
2 Puls M, Beuthner BE, Topci R, *et al*. Impact of myocardial fibrosis on left ventricular remodelling, recovery, and outcome after transcatheter aortic valve implantation in different haemodynamic subtypes of severe aortic stenosis. *Eur Heart J* 2020;41:1903–14.
3 Ross J. Afterload mismatch and preload reserve: a conceptual framework for the analysis of ventricular function. *Prog Cardiovasc Dis* 1976;18:255–64.
4 Ross J. Afterload mismatch in aortic and mitral valve disease: implications for surgical therapy. *J Am Coll Cardiol* 1985;5:811–26.
5 Liebenberg J, Doubell AF, Steyn J, *et al*. Exploring the mechanisms responsible for reduced systolic function in high-gradient aortic stenosis. *Heart* 2023;109:1858–63.
6 Krayenbuehl HP, Hess OM, Monrad ES, *et al*. Left ventricular myocardial structure in aortic valve disease before, intermediate, and late after aortic valve replacement. *Circulation* 1989;79:744–55.
7 Hein S, Arnon E, Kostin S, *et al*. Progression from compensated hypertrophy to failure in the pressure-overloaded human heart: structural deterioration and compensatory mechanisms. *Circulation* 2003;107:984–91.
8 Bing R, Cavalcante JL, Everett RJ, *et al*. Imaging and Impact of Myocardial Fibrosis in Aortic Stenosis. *JACC Cardiovasc Imaging* 2019;12:283–96.
9 Calin A, Mateescu AD, Popescu AC, *et al*. Role of advanced left ventricular imaging in adults with aortic stenosis. *Heart* 2020;106:962–9.
10 Kong P, Christia P, Frangogiannis NG. The pathogenesis of cardiac fibrosis. *Cell Mol Life Sci* 2014;71:549–74.
11 Vahanian A, Beyersdorf F, Praz F. Corrigendum to: 2021 ESC/EACTS Guidelines for the management of valvular heart disease: Developed by the Task Force for the management of valvular heart disease of the European Society of Cardiology (ESC) and the European Association for Cardio-Thoracic Surgery (EACTS). *Eur Heart J* 2022;43:2022.
12 Kramer CM, Barkhausen J, Flamm SD, *et al*. Standardized cardiovascular magnetic resonance (CMR) protocols 2013 update. *J Cardiovasc Magn Reson* 2013;15:91.
13 Schulz-Menger J, Bluemke DA, Bremerich J, *et al*. Standardized image interpretation and post-processing in cardiovascular magnetic resonance - 2020 update. *J Cardiovasc Magn Reson* 2020;22:19.
14 Reichek N, Wilson J, St John Sutton M, *et al*. Noninvasive determination of left ventricular end-systolic stress: validation of the method and initial application. *Circulation* 1982;65:99–108.
15 Carter-Storch R, Moller JE, Christensen NL, *et al*. End-systolic wall stress in aortic stenosis: comparing symptomatic and asymptomatic patients. *Open Heart* 2019;6:e001021.
16 Mewton N, Opdahl A, Choi E-Y, *et al*. Left ventricular global function index by magnetic resonance imaging--a novel marker for assessment of cardiac performance for the prediction of cardiovascular events: the multi-ethnic study of atherosclerosis. *Hypertension* 2013;61:770–8.
17 Cerquiera MD, Weissman NJ, Dilsizian V, *et al*. Standardized myocardial segmentation and nomenclature for tomographic imaging of the heart: a statement for healthcare professionals from the cardiac imaging committee of the council on clinical cardiology of the American Heart Association. *Circulation* 2002;105:539–42.
18 Flett AS, Hayward MP, Ashworth MT, *et al*. Equilibrium contrast cardiovascular magnetic resonance for the measurement of diffuse myocardial fibrosis: preliminary validation in humans. *Circulation* 2010;122:138–44.
19 Opatril L, Panovsky R, Machal J, *et al*. Extracellular volume quantification using synthetic haematocrit assessed from native and post-contrast longitudinal relaxation T1 times of a blood pool. *BMC Cardiovasc Disord* 2021;21:363.
20 Treibel TA, López B, González A, *et al*. Reappraising myocardial fibrosis in severe aortic stenosis: an invasive and non-invasive study in 133 patients. *Eur Heart J* 2018;39:699–709.
21 Carabello BA, Green LH, Grossman W, *et al*. Hemodynamic determinants of prognosis of aortic valve replacement in critical aortic stenosis and advanced congestive heart failure. *Circulation* 1980;62:42–8.
22 Croke RP, Pifarre R, Sullivan H, *et al*. Reversal of advanced left ventricular dysfunction following aortic valve replacement for aortic stenosis. *Ann Thorac Surg* 1977;24:38–43.
23 Smith N, McAnulty JH, Rahimtoola SH. Severe aortic stenosis with impaired left ventricular function and clinical heart failure: results of valve replacement. *Circulation* 1978;58:255–64.
24 Everett RJ, Tastet L, Clavel M-A, *et al*. Progression of Hypertrophy and Myocardial Fibrosis in Aortic Stenosis: A Multicenter Cardiac Magnetic Resonance Study. *Circ Cardiovasc Imaging* 2018;11:e007451.
25 Treibel TA, Fontana M, Kozor R, *et al*. Diffuse myocardial fibrosis - a therapeutic target? Proof of regression at 1-year following aortic valve replacement: the RELIEF-AS study. *J Cardiovasc Magn Reson* 2016;18:O37.

26 Neff LS, Zhang Y, Van Laer AO, *et al*. Mechanisms that limit regression of myocardial fibrosis following removal of left ventricular pressure overload. *Am J Physiol Heart Circ Physiol* 2022;323:H165–75.
27 Treibel TA, Kozor R, Schofield R, *et al*. Reverse Myocardial Remodeling Following Valve Replacement in Patients With Aortic Stenosis. *J Am Coll Cardiol* 2018;71:860–71.
28 Loganath K, Craig NJ, Everett RJ, *et al*. Early Intervention in Patients With Asymptomatic Severe Aortic Stenosis and Myocardial Fibrosis: The EVOLVED Randomized Clinical Trial. *JAMA* 2025;333:213–21.
29 Mutlak D, Aronson D, Lessick J, *et al*. Frequency, characteristics, and outcome of patients with aortic stenosis, left ventricular dysfunction, and high (versus low) trans-aortic pressure gradient. *Isr Med Assoc J* 2010;12:563–7.
30 Ternacle J, Faroux L, Alperi A, *et al*. Impact of Left-Ventricular Dysfunction in Patients With High- and Low- Gradient Severe Aortic Stenosis Following Transcatheter Aortic Valve Replacement. *Can J Cardiol* 2021;37:1103–11.
31 Naicker A, Brown S, Ponnusamy S. Outcomes following aortic valve replacement for isolated aortic stenosis with left ventricular dysfunction. *SAHJ* 2016;13:290–6.
32 Nwabuo CC, Moreira HT, Vasconcellos HD, *et al*. Left ventricular global function index predicts incident heart failure and cardiovascular disease in young adults: the coronary artery risk development in young adults (CARDIA) study. *Eur Heart J Cardiovasc Imaging* 2019;20:533–40.
33 Eitel I, Pöss J, Jobs A, *et al*. Left ventricular global function index assessed by cardiovascular magnetic resonance for the prediction of cardiovascular events in ST-elevation myocardial infarction. *J Cardiovasc Magn Reson* 2015;17:62.